Drag on Spheres

Prepared by Professor J. M. Cimbala, Penn State University
Latest revision: 11 January 2012

Nomenclature

a	speed of sound
A	projected frontal area (for a sphere, $A = \pi d^2/4$)
C_D	drag coefficient: $C_D = 2F_D/(\rho V^2 A)$
C_L	lift coefficient: $C_L = 2F_L/(\rho V^2 A)$
d	diameter of a cylinder, sphere, or other object
F_D	drag force
F_L	lift force
g	gravitational constant (9.81 m/s^2)
L	characteristic length of a body (for a sphere, $L = d$)
m	mass
Ma	Mach number: Ma = V/a
P	static pressure
P_{atm}	atmospheric pressure
P_T	total or stagnation pressure
R	specific ideal gas constant: for air, R = 287. m^2/(s^2·K)
Re_d	Reynolds number based on diameter d: $\text{Re}_d = Vd/\nu$ (other Reynolds numbers defined similarly)
t	time
T_{amb}	ambient air temperature
V	mean freestream velocity in the test section of the wind tunnel
ε	average surface roughness height on the surface of a body
μ	coefficient of dynamic viscosity (also called simply the viscosity)
ν	coefficient of kinematic viscosity (for water, $\nu \approx 1.0 \times 10^{-6}$ m^2/s at room temperature)
ρ	density of the fluid (for water, $\rho \approx 998$ kg/m^3 at room temperature)

Educational Objectives

1. Develop familiarity with operation of a wind tunnel, Pitot-static probe, electronic pressure transducer, water manometer, and electronic drag balance.
2. Reinforce knowledge of the usefulness of dimensional analysis.
3. Observe the "drag crisis" associated with a sphere at high Reynolds numbers, and the effect of surface roughness on sphere drag.
4. Measure the drag coefficient of a model car for several configurations, and compare.

Equipment

1. high speed undergraduate wind tunnel
2. Validyne electronic pressure transducer and digital manometer, Model CD23
3. Meriam micro manometer, Model SC-2897, with hand pressure pump
4. Measurements Group, Inc. strain indicator, Model 3800
5. TSI integrating voltmeter, Model 1076
6. Techkor data unit, Model MEPTS-9000, with thermocouple module
7. barometric pressure gauge (mounted on the wind tunnel to the left of the test section)
8. glass thermometer and thermocouple thermometer
9. ruler
10. strain gage drag and lift balance, with removable sting mount (threads on the sting mount are 1/4-20)
11. drag balance calibration stand, with Ohaus 10-1000 gram weight set
12. personal computer with digital data acquisition system, data acquisition software
13. United Sensors Pitot-static probe (mounted upstream of model in freestream), with traverse and stand
14. spheres of various sizes and roughness, as indicated on the following chart (*Note*: These are also posted on the wind tunnel wall for your convenience.):

Description of sphere (some of these spheres may not be available in the lab)	**Sphere diameter, *d* (inches)**	**Projected frontal area, *A* (square inches)**
golf balls:		
smooth white golf ball (no dimples)	1.68	2.22
Titleist	1.67	2.19
Topflite XL	1.68	2.22
Makfli HT	1.68	2.22
Penn State	1.69	2.24
Magna	1.71	2.30
small smooth yellow-orange ball	2.83	6.29
small roughened yellow-orange ball	2.83	6.29
baseball	2.84	6.33
small smooth brass ball	2.97	6.93
softball	3.77	11.16
medium smooth brass ball	3.84	11.58
large smooth brass ball	4.98	19.48

Background

Wind tunnels are widely used in industry and research to simulate the flow around an object (such as an automobile, airplane, etc.) traveling through the air. In many cases, the model to be tested in the wind tunnel is not the same size as the prototype. The freestream velocities may differ as well. It is therefore desirable to match the Reynolds number of the model to that of the prototype. This is not always possible in a small wind tunnel like ours, but fortunately many parameters are nearly constant over a wide range of Reynolds number.

The drag force on a sphere is a classic example. As seen in Figure 1 (reproduced from Reference 1), drag coefficient C_D is relatively flat in the range of Reynolds number between about 10^3 and 2×10^5. In this range, therefore, C_D can be considered nearly independent of Re_d. At higher Reynolds numbers however, the drag coefficient drops suddenly from a value between 0.4 and 0.5 at $\mathrm{Re}_d = 2 \times 10^5$ to a value slightly below 0.1 at $\mathrm{Re}_d = 4 \times 10^5$. This sudden drop in C_D is called the "drag crisis", which is associated with separation of the boundary layer from the surface of the sphere. Namely, for $\mathrm{Re}_d < 2 \times 10^5$ the boundary layer on the forward portion of the sphere is laminar. This boundary layer separates just upstream of the sphere midsection, leading to a very wide wake and large drag. For a smooth sphere, as Re_d increases beyond 2×10^5, the laminar boundary layer begins to transition into a turbulent boundary layer on the forward surface. Since a turbulent boundary layer is more resistant to flow separation than is a laminar boundary layer, the turbulent boundary layer remains attached to the sphere surface for a longer distance around the sphere, separating well downstream of the sphere midsection. The resulting wake is much narrower, with a corresponding lower drag.

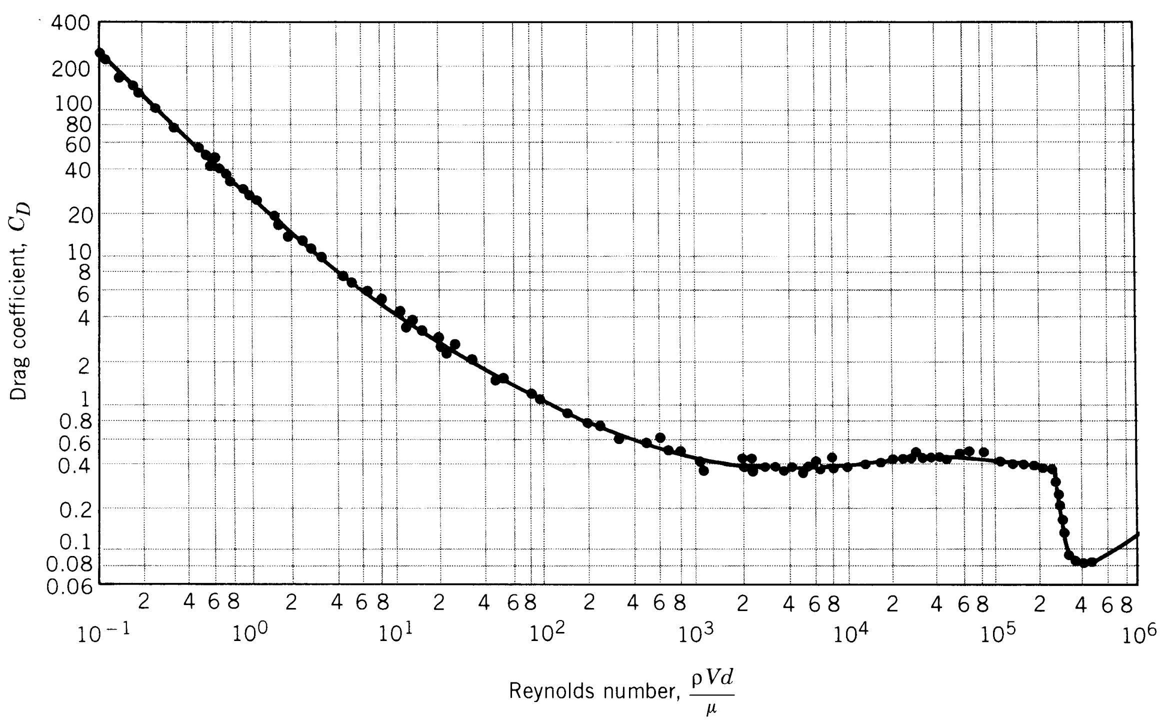

Figure 1. Effect of Reynolds number on the drag coefficient of a smooth sphere

Spheres or balls are used in many sports. Oftentimes it is desirable to have a very low drag coefficient so that the ball can travel faster through the air. For cases where the Reynolds number is not high enough for the drag crisis to occur naturally, artificial roughness is often added to the sphere surface. Examples in sports include the dimples on golf balls and the threaded seams on baseballs and softballs. Flow disturbances due to the roughness cause premature transition of the boundary layer from laminar to turbulent, and the drag crisis can be forced to occur at a Reynolds number significantly lower than that 2×10^5, as shown in Figure 2, also taken from Reference 1.

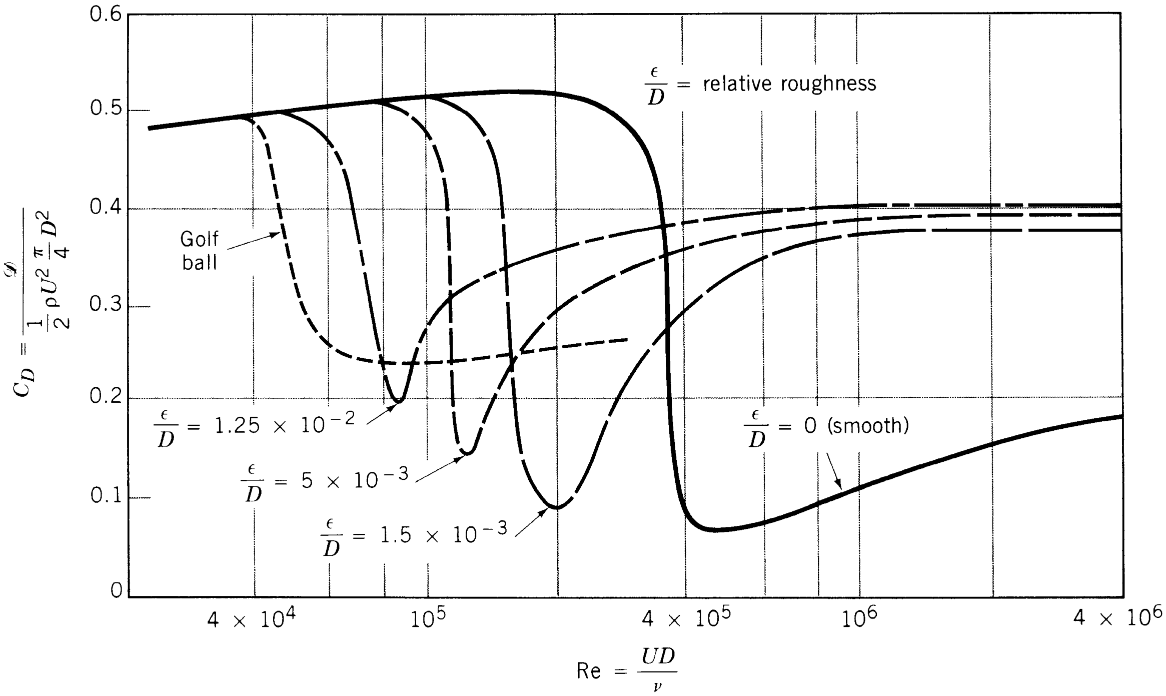

Figure 2. Effect of surface roughness on the drag coefficient of a sphere

In this lab experiment you will measure the drag of spheres as a function of both sphere diameter and wind tunnel speed. Dimensional analysis will enable you to normalize your data onto one curve. The effect of surface roughness will also be explored.

References

1. Munson, B. R., Young, D. F., and Okiishi, T. H., *Fundamentals of Fluid Mechanics*, Wiley, NY, 1990.
2. Çengel, Y. A. and Cimbala, J. M., *Fluid Mechanics – Fundamentals and Applications*, McGraw-Hill, NY, 2006.
3. White, F. M., *Fluid Mechanics*, Ed. 5, McGraw-Hill, NY, 2003.